



**HAL**  
open science

## Study of the physicochemical interactions of nanoformulations based on polyoxazolines with a skin surface model

L. Simon, C. Picard, L.S. Calixto, Vincent Lapinte, J.M. Devoisselle, S. Bégu

► **To cite this version:**

L. Simon, C. Picard, L.S. Calixto, Vincent Lapinte, J.M. Devoisselle, et al.. Study of the physicochemical interactions of nanoformulations based on polyoxazolines with a skin surface model. *Colloids and Surfaces A: Physicochemical and Engineering Aspects*, 2021, 626, pp.127027. 10.1016/j.colsurfa.2021.127027 . hal-03334558

**HAL Id: hal-03334558**

<https://hal.umontpellier.fr/hal-03334558v1>

Submitted on 2 Aug 2023

**HAL** is a multi-disciplinary open access archive for the deposit and dissemination of scientific research documents, whether they are published or not. The documents may come from teaching and research institutions in France or abroad, or from public or private research centers.

L'archive ouverte pluridisciplinaire **HAL**, est destinée au dépôt et à la diffusion de documents scientifiques de niveau recherche, publiés ou non, émanant des établissements d'enseignement et de recherche français ou étrangers, des laboratoires publics ou privés.



Distributed under a Creative Commons Attribution - NonCommercial 4.0 International License

# Study of the physicochemical interactions of nanoformulations based on polyoxazolines with a skin surface model

L. Simon<sup>1</sup>, C. Picard<sup>2\*</sup>, L. S. Calixto<sup>2</sup>, V. Lapinte<sup>1</sup>, J.M. Devoisselle<sup>1</sup>, S. Bégu<sup>1\*</sup>

1: ICGM, Montpellier University, CNRS, ENSCM, Montpellier, France

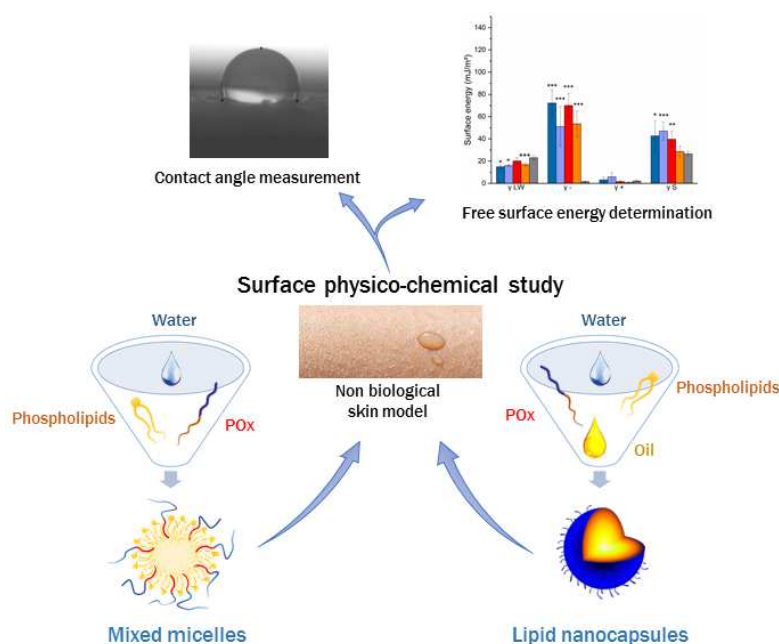
2: Normandie Univ, UNILEHAVRE, FR 3038 CNRS, URCOM, EA 3221, France

## Abstract

The behavior of polyoxazolines based mixed micelles and lipid nanocapsules on skin surface was studied on nonbiological human skin surface model to assess the formulations potential for topical delivery. Two amphiphilic polyoxazolines, saturated ( $C_{16}POx_{15}$ ) and unsaturated ( $C_{18:2}POx_{15}$ ), were used to evaluate the polymer architecture impact on formulations interaction with skin surface. To do so, the formulations spontaneous spreading and their residual film left on surface after manual application was investigated using contact angle measurements and free surface energy determination. The Van Oss model was employed to identify the physicochemical interactions in order to understand how the formulations can change the skin surface properties. In brief, both formulations showed a good affinity with the surface but depending on the polyoxazoline used, the spontaneous formulation spreading was modulated. Overall, the residual film left on the model surface modified the skin model physicochemical properties leading to a better interaction with hydrophilic and polar compounds. Regarding in detail each excipient impact on the surface physicochemical properties further explained the resulting formulation behavior on the skin surface model and highlighted the crucial role of the main component.

**Key words:** Skin surface model, physicochemical properties, polyoxazoline, lipid nanocapsule, mixed micelles, free surface energy, contact angle

## Graphical abstract



29  
30

## 31 I.1 Introduction

32 To protect the human body from external aggressions, the skin acts as a shield. More especially, the  
33 *stratum corneum* with its unique composition and structure of corneocytes embedded in lipid matrix  
34 such as “brick and mortar” ensures stiffness and protection [1]. The external aggressions defined as  
35 “skin exposome” [2] (pollution, cigarette smoke, UV) directly impact the skin by inducing increased  
36 production of radical oxygen species (ROS). Overall, the excess of ROS accelerated skin aging and  
37 higher risks of skin cancer [3]. To help the skin maintains its essential integrity for its barrier function,  
38 topical products are proposed to deliver active ingredients and to prevent skin damages from  
39 happening. Once applied on the skin, topical product spreads onto the surface and then interacts  
40 with the skin surface components mainly the sebum. Therefore, it is of interest to predict and  
41 understand how the product interacts and modifies the skin surface properties to enhance  
42 penetration. To do so, a method was developed based on physicochemical interactions and free  
43 surface energy of the skin surface determination. Van Oss et al. studied the interactions of Lifshitz-  
44 Van der Waals gathering the forces of Keesom (orientation), Debye (induction) and London  
45 (dispersion) and the interactions acide-base (electron acceptor and electron donor, respectively) to  
46 characterize the interfacial energy [4]. Mavon et al. applied this equation model to study the effect of  
47 sebum on human skin and proved that skin behaves like a basic monopolar surface and sebum  
48 increases its hydrophilic affinity (strong electron donor component) [5],[6].

49 Therefore, Van Oss model and method can predict the spreading and affinity of the topical product  
50 on the skin. However, to avoid toxic hazard during *in vivo* testing or wasting expensive *ex vivo* skin,  
51 nonbiological skin models (NBSM) were fine tuned to mimic the skin surface properties. Eudier et al.  
52 previously deeply examined some nonbiological model regarding their physicochemistry [7] and  
53 patented a model reproducing the skin topography and sebum composition. A correlation between  
54 the tested solution on their model and *in vivo* results was established [8].

55 Thus, this NBSM was selected to investigate the surface interactions with new lipid nanoformulations  
56 based on amphiphilic polyoxazolines. Polyoxazoline (POx) is a bioinspired nonionic polymer with a  
57 risen interest for therapeutic use due to its excellent biomedical properties [9]. The hydrophilic POx  
58 was associated with lipid alkyl chain to form amphiphilic POx also called LipoPOx [10]. The LipoPOx  
59 will be called POx in this article to ease the comprehension of the study. Various POx were  
60 investigated for their interesting features in development of nanodrug delivery systems and many  
61 were developed for intravenous injection delivery. However, POx was also formulated for skin  
62 delivery in lipid based nanoformulations such as liposomes, mixed micelles (MM) [11] and lipid  
63 nanocapsules (LNC) [12] as stabilizing agent and potential penetration enhancer. MM and LNC were  
64 proved to encapsulate, protect and deliver while maintaining the molecule bioactivity in our case a  
65 strong antioxidant: quercetin. These two formulations have different composition and morphology  
66 suggesting divergent behavior. MM is composed of phospholipids and POx with a hydrophobic core  
67 made of the entanglement of hydrophobic chains. On the contrary, LNC is highly ordered with an oily  
68 core surrounded by a phospholipid rigid capsule and POx corona. The resulting nanoscale mechanical  
69 properties might influence the interaction with the NBSM. Now, as POx have never been used for  
70 topical delivery, our work evaluates the MM and LNC interactions with the NBSM and to characterize  
71 the free surface energy. Two different POx, one with a linear saturated and one with a linear  
72 unsaturated alkyl chain, were explored to see if one of them leads to better skin affinity and  
73 penetration efficiency. To go further into understanding the surface physicochemistry, each  
74 component of the two formulations will be investigated such as POx.

## 75 I.2 Materials and Methods

76 -For POx synthesis:

77 2-Methyl-2-oxazoline (MOx, Sigma Aldrich, 99.0%) was dried over CaH<sub>2</sub>, distilled at reduced pressure  
78 and stored under nitrogen atmosphere. Iodo-hexadecane (95.0 %), potassium hydroxide (KOH),  
79 lithium aluminum hydride (LiAlH<sub>4</sub>, 95 %), trimethylamine (98 %), methanesulfonyl chloride (99.7 %)  
80 acetonitrile, diethyl ether, anhydrous tetrahydrofuran (99 %), methanol and acetone were bought  
81 from Sigma Aldrich (Germany). Linseed oil was brought from Bioplanète (France).

82 -For POx based nanoformulations:

83 Phosphatidylcholine (L- $\alpha$ -Phosphatidylcholine from egg yolk  $\approx$  60%) and Brij®58 were purchased from  
84 Sigma Aldrich (Sigma Aldrich, Germany). Lipophilic Labrafac® WL 1349 (caprylic/capric triglycerides)  
85 was brought from Gattefossé (France) and Lipoid S75 (soybean phospholipids with 70%  
86 phosphatidylcholine) was kindly provided by Lipoid (Germany). Sodium chloride (NaCl) was bought  
87 from VWR. MilliQ water was produced from Milli-Q Gradient A10 (Merck Millipore, Germany)  
88 apparatus.

89 -For contact angle measurements:

90 Three reference liquids were used to perform surface free energy calculations: ultrapure water  
91 (resistivity of 18 M $\Omega$ .cm<sup>-1</sup> at 25 °C) from Merck Millipore (Germany), diiodomethane (analytical  
92 grade, 99% purity) and formamide (analytical grade, 99% purity) from Sigma Aldrich (Germany).

93

### 94 I.2.1 Amphiphilic polyoxazolines (POx) synthesis: C<sub>16</sub>POx<sub>n</sub> and C<sub>18:2</sub>POx<sub>n</sub>

95 Both polyoxazolines (POx) syntheses were based on cationic ring-opening polymerization of MOx  
96 performed under nitrogen atmosphere.

97 The polymerization of C<sub>16</sub>POx<sub>n</sub> was initiated with the commercialized iodohexadecane. Regarding  
98 C<sub>18:2</sub>POx<sub>n</sub>, the initiator of the polymerization was produced from the linseed oil in two steps. First the  
99 linseed oil (4 g, 4.55 mmol) was reduced by lithium aluminum hydride (9 eq, 41 mmol) under  
100 nitrogen atmosphere in dry tetrahydrofuran for 8 h. The organic phase was then solubilized in  
101 dichloromethane and washed with a solution of sodium chloride saturated. The corresponding fatty  
102 alcohol (NMR spectra Figure SI 1) was obtained with a yield of 98 %. Then, methanesulfonyl chloride  
103 (1.5 eq, 22.5 mmol) and trimethylamine (1.5 eq, 22.5 mmol) were added to the fatty alcohol in dry  
104 diethyl ether for 8 h. After washing with water and dried on MgSO<sub>4</sub>, the initiator of the  
105 polymerization (C<sub>18:2</sub>OMs) was synthesized (NMR spectra Figure SI 2) with a yield of 93 %.

106 C<sub>16</sub>POx<sub>n</sub> was synthesized after dissolving iodohexadecane (3.564 g, 10.1 mmol) and MOx (15 eq,  
107 151.7 mmol) in dry acetonitrile (0.5 M). After strong agitation at 80 °C for 8 h, the solution was  
108 quenched with potassium hydroxide dissolved in methanol (5 eq, 50.5 mmol, 5M). The mixture was  
109 left under magnetic stirring at 40 °C for 8 h. The C<sub>16</sub>POx<sub>15</sub> was obtained after precipitation dropwised  
110 in cold diethyl ether and filtration [11]. C<sub>16</sub>POx<sub>15</sub> had a molar mass of 1500 g/mol and a critical  
111 aggregation concentration of respectively 150 mg/L. C<sub>18:2</sub>POx<sub>15</sub> synthesis occurred in the same  
112 conditions with the initiator (C<sub>18:2</sub>OMs) (2.5 g, 7.8 mmol) left to react with MOx (15 eq, 117 mmol) in  
113 dry acetonitrile (0.5 M). The polymerization and purification conditions remained the same as  
114 C<sub>16</sub>POx<sub>15</sub>. C<sub>18:2</sub>POx<sub>15</sub> (NMR spectra Figure SI 3) had a molar mass of 1500 g/mol and a critical  
115 aggregation concentration of respectively 100 mg/L.

116 The HLB of both polyoxazoline was calculated based on the Griffin method adapted for nonionic  
117 surfactant as the equation:

$$118 \quad \frac{\text{molar mass of hydrophilic part}}{\text{total molar mass}} \times 20$$

119

### 120 **1.2.2 Preparation of mixed micelles (MM)**

121 The mixed micelles (MM) were produced using the thin film method with POx and  
122 phosphatidylcholine (PC) at the molar ratio 1:40. The components were dissolved in chloroform:  
123 acetone in 1:1 volume ratio and the film was made after evaporation of the solvent mixture under  
124 vacuum at 40 °C. The film of PC and POx was hydrated with filtered phosphate buffered saline (PBS,  
125 150 mM, pH 7.4). The solution was then processed 5 times with a high pressure homogenizer  
126 (Microfluidizer LV1, Microfluidics, USA) at 10 000 PSI. The size of MM was measured with a Zetasizer  
127 NanoZS apparatus (Malvern Instrument, UK) at 18 nm (PDI 0.3). Further structural characterization  
128 such as TEM and DSC as well as stability study were performed in [11].

129 To evaluate the impact of PC excipient on the nonbiological skin model surface properties, the  
130 phospholipids were prepared as liposome at the same concentration as in MM (10 g/L).

### 131 **1.2.3 Preparation of lipid nanocapsules (LNC)**

132 The lipid nanocapsules (LNC) were composed of POx (200 mg), caprylic acid triglycerides oil  
133 (Labrafac®) (150 mg) and water (650 mg) and additional phospholipids (Lipoid® S75) (15 mg) and  
134 NaCl (30 mg). The mixture was heated at 85 °C and cooled down to 30 °C three times and then  
135 sonicated for 4 min at 30 % amplitude with a sonication probe (Branson Ultrasonics Corporation,  
136 USA). The solution was heated and cooled down again and 2.5 mL of cold water was added under  
137 magnetic stirring. The resulting LNC size was about 30 nm and a PDI of 0.16 [12]. Further structural  
138 characterization such as TEM and AFM as well as stability study were performed in [12].

139

140 To evaluate the impact of S75 excipient on the nonbiological skin model surface properties, the  
141 phospholipids were prepared as liposome at the same concentration as in LNC (5 g/L).

### 142 **1.2.4 Nonbiological skin surface model**

143 The model was developed by Eudier et al. and the production of the NBSM was deeply explained in  
144 their article [8]. The NBSM was made of two parts, one polymeric material (biocompatible silicon)  
145 mimicking the surface topography and a coating of artificial sebum (28% free fatty acids, 32%  
146 triglycerides, 25% was esters, 10% squalene and 4% cholesterol) reproducing the lipid composition of  
147 skin face.

### 148 **1.2.5 Advancing contact angle measurement**

149 The contact angles were measured with a portative goniometer (PGX +, ScanGaule, France)  
150 associated to a high resolution camera and connected to a software (PGPlus). A syringe with an  
151 internal diameter of 0.77 mm was used to deposit the solution droplet on the surface. Five  
152 successive droplet deposition were performed to reach a final volume of droplet of 7 µL to measure  
153 the advancing contact angle. Five pictures were taken immediately after each deposition. Contact  
154 angles were determined with the software on both sides of the droplet, the maximum value of the

155 two sides mean from the five measurements was selected. This entire measurement procedure was  
 156 repeated five times for each solution tested on the NBSM. All measurements were conducted at 20  
 157 °C.

158 The kinetics measurement over 5 minutes was performed with the same protocol. After deposition, a  
 159 picture was taken every minute. The same kinetic measurement was performed with water and no  
 160 significant modification of contact angle was observed showing that the evaporation is neglected.

### 161 **I.2.6 Free surface energy determination**

162 To determine the free surface energy, 20 µL of solution were dropped on the NBSM surface of 5 cm<sup>2</sup>  
 163 and spread manually with 15 rotations and left untouched for 3 minutes. Contact angles with water,  
 164 diiomethane and formamide were performed with the same procedure as described in 2.5. The Van  
 165 Oss was employed to determine the free surface energy using the Lifschitz-Van Der Waals ( $\gamma_{LW}$ )  
 166 components (interactions Keesom, Debye, London) and acid-base components (electron acceptor  $\gamma^+$   
 167 and electron donor  $\gamma^-$ ) [5], [4]. Each component was determined with the following Young equation:

$$168 \quad (1 + \cos \theta)\gamma_L = 2\sqrt{\gamma_L^{LW}\gamma_S^{LW}} + 2\sqrt{\gamma_L^+\gamma_S^-} + 2\sqrt{\gamma_L^-\gamma_S^+}$$

169 The determination of this equation is further explained in Eudier et al. article [8].

### 170 **I.2.7 Statistical analysis**

171 The statistical analysis of the data conducted on the contact angles and free surface energy were  
 172 performed using the Origin Pro software 8.1 (OriginLab, USA). A two-sample t-test with equal  
 173 variance was carried out to compare results one by one. The P value reflects the significance with \*P  
 174 < 0.05, \*\*P < 0.01 and \*\*\*P < 0.001.

175

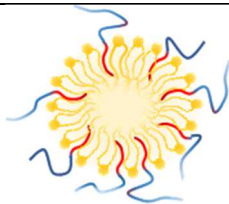
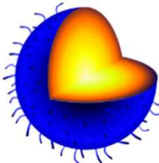
## 176 **I.3 Results and discussion**

### 177 **I.3.1 Presentation of the mixed micelles and lipid nanocapsules**

178 In order to understand the interactions of the MM and LNC with the surface of NBSM, the main  
 179 features of the formulations are summarized in Table 1. This table reflected the difference of  
 180 composition and morphology of the two formulations. MM is mainly composed of phospholipids  
 181 whereas LNC has more POx and oil. Regarding their morphology, the hydrophobic core of MM  
 182 correspond to the entanglement of phospholipids and POx alkyl chains [11] whereas for LNC, it is a  
 183 rigid capsule of phospholipids and POx and a soft oil core. The mechanical properties due to the rigid  
 184 capsule of LNC were confirmed with no deformation observed up to a constraint of 10-20 nN [12].

185

*Table 1: Composition and concentration of MM and LNC*

	Mixed micelles	Lipid nanocapsules
<b>Structure</b>		
<b>Size (PDI)</b>	20 nm (0.30)	30 nm (0.16)

Name	Composition	Concentration (g/L)	Name	Composition	Concentration (g/L)
<b>Liposome PC</b>	Phosphatidylcholine	10	<b>Liposome S75</b>	70% Phosphatidylcholine + 30% soy bean lecithin	5
<b>POx</b>	C <sub>16</sub> POx <sub>15</sub> or C <sub>18:2</sub> POx <sub>15</sub>	0.5	<b>POx</b>	C <sub>16</sub> POx <sub>15</sub> or C <sub>18:2</sub> POx <sub>15</sub>	62.5
			<b>Labrafac®</b>	Caprylic/ capric triglycerides	48

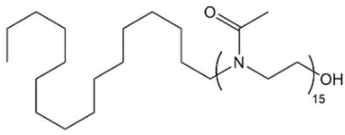
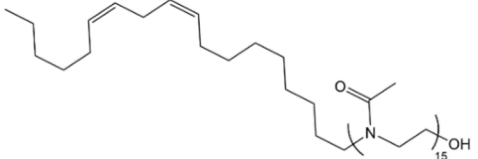
186

187 The characteristics of the two POx polymers: structure, molar mass, CMC, calculated HLB are  
 188 summarized in Table 2 to evaluate the impact of the alkyl chain of the two different POx in  
 189 formulation. These features were determined as described in a previous publication [11]. Even if  
 190 their structures are different, their properties do not differ a lot. The other components such as the  
 191 excipients used in the formulations were then examined as described in Table 1.

192

193

*Table 2: Summary of C<sub>16</sub>POx<sub>15</sub> and C<sub>18:2</sub>POx<sub>15</sub> characteristics*

Properties	C <sub>16</sub> POx <sub>15</sub>	C <sub>18:2</sub> POx <sub>15</sub>
<b>Structure</b>		
<b>Molar mass (g/mol)</b>	1520	1540
<b>CMC (mg/L)</b>	150	100
<b>Effectiveness (mN/m)</b>	34	32
<b>Calculated HLB</b>	17	16.7

194

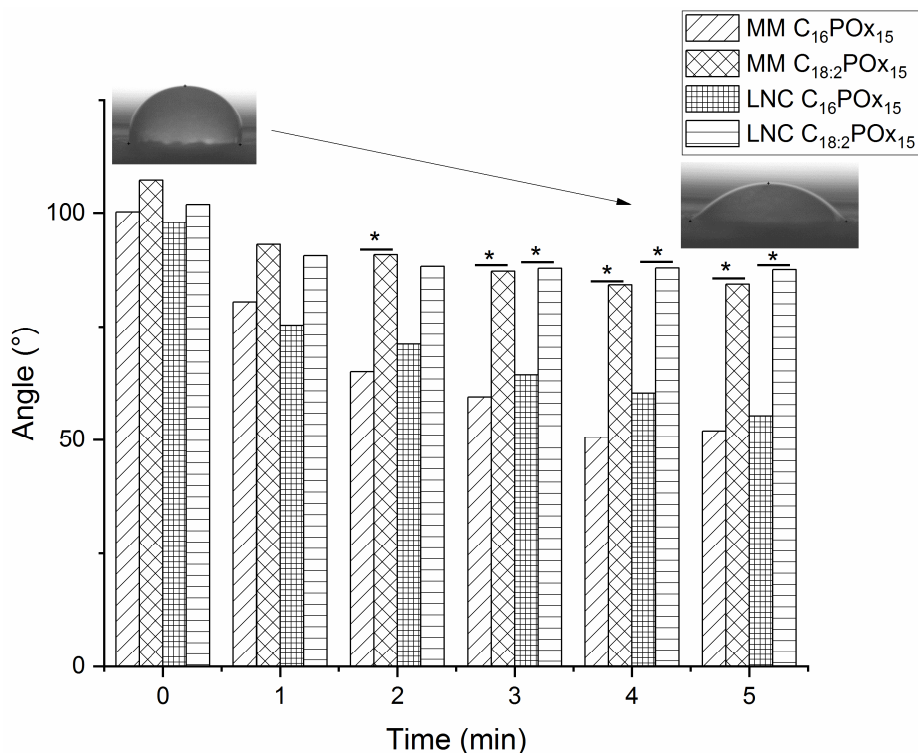
### 195 1.3.2 Interactions of mixed micelles and lipid nanocapsules with the NBSM model

196 The contact angle of the two formulations on the NBSM was measured from 0 to 5 minutes to  
 197 evaluate the spontaneous spreading of the solution on the surface after a droplet deposition and the  
 198 potential kinetic effect over 5 minutes (Figure 1). Contact angle measurements characterize the  
 199 wettability of a surface by a liquid which depends on the intermolecular interaction between the  
 200 two. Thus, the smaller the angle is, the higher the liquid spreads, indicating a better intermolecular  
 201 interaction.

202 The NBSM mimicking the physicochemical properties of the surface of the skin behaves as a basic  
 203 monopolar surface. The contact angle of water is about 100° reflecting the hydrophobic surface  
 204 properties of NBSM and confirming the properties of the model as in [8]. At T0, just after deposition  
 205 on the NBSM all formulations behaved as water (due to the aqueous continuous medium) with a  
 206 contact angle of about 100°. Afterwards, a kinetic effect occurred during the first minutes with a  
 207 sharp decrease of the contact angle for formulations with C<sub>16</sub>POx<sub>15</sub> (50° for MM and 55° for LNC) and  
 208 with a slight decrease for C<sub>18:2</sub>POx<sub>15</sub> (84° for MM and 87° for LNC). After 3 minutes, a plateau was

209 reached. A contact angle lower than 90° implies that the formulation has affinity with the surface.  
 210 From this plateau, a significant difference between the two formulated POx was demonstrated but  
 211 none between the type of formulations. To conclude, the POx alkyl chain rapidly dominates over the  
 212 formulations effect or concentration of POx. Formulations with C<sub>16</sub>POx<sub>15</sub> reacted quickly with the  
 213 surface reflecting their affinity and leading to an enhanced spreading whereas C<sub>18:2</sub>POx<sub>15</sub> had almost  
 214 no impact.

215



216

217

218 *Figure 1: Contact angle of MM and LNC with C<sub>16</sub>POx<sub>15</sub> and C<sub>18:2</sub>POx<sub>15</sub> over 5 minutes after deposition on the*  
 219 *NBSM. Statistical analysis was performed by a two-sample t-test between the same formulation with different*  
 220 *POx (\*P < 0.05)*

221 To get rid of the kinetic effect and understand the interactions, the formulations were manually  
 222 spread on the NBSM according to the procedure described. The surface was covered with a  
 223 formulation residual film and left untouched for 3 minutes. It was noticed that the spreading was not  
 224 completely homogenous on the surface as it is the case *in vivo* for application of aqueous products  
 225 on human skin. This might be explained by the weak interaction of the hydrophobic surface with a  
 226 hydrophilic water based solutions in addition to the lack of adsorption due to the polymeric nature of  
 227 the NBSM. The total surface energy ( $\gamma_s$ ) was composed of 3 components ( $\gamma_{LW}$ ,  $\gamma^+$ ,  $\gamma^-$ ) (Figure 2). The  
 228 surface energy of the NBSM with no formulation applied was measured and considered as a  
 229 reference for statistical analysis.

230 The residual film after application on the NBSM was first characterized as described [8], after 3  
 231 minutes looking at the water contact angle. Before any product application, the NBSM had a water  
 232 angle of  $114.6 \pm 1.7^\circ$  whereas after formulations application, the value decreased as follows: LNC  
 233 C<sub>16</sub>POx<sub>15</sub> ( $41.2 \pm 4.2^\circ$ ) > LNC C<sub>18:2</sub>POx<sub>15</sub> ( $38.8 \pm 2.3^\circ$ ) > MM C<sub>18:2</sub>POx<sub>15</sub> ( $35.2 \pm 4.9^\circ$ ) > MM C<sub>16</sub>POx<sub>15</sub> ( $32.5$   
 234  $\pm 4.9^\circ$ ). The residual film obtained after spreading both formulations deeply modified the surface

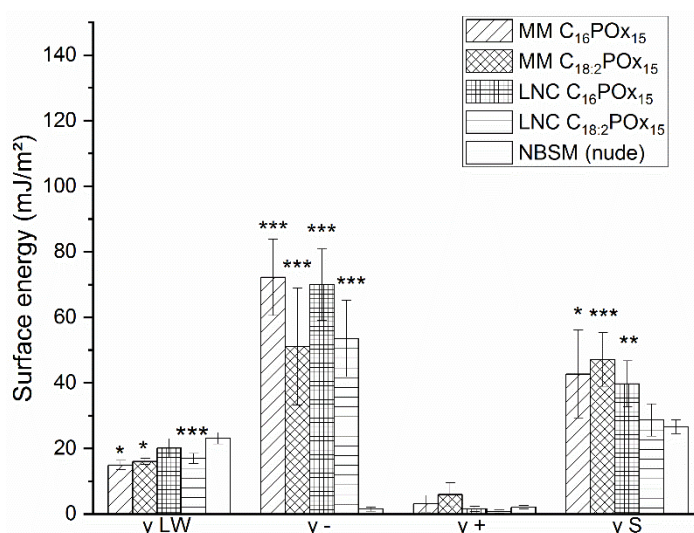


235 properties as Eudier et al. have previously described with standard emulsion [8]. The free surface  
 236 energy might help understanding the ongoing interactions. All the following modifications were  
 237 proved to be significant.

238 The total surface energy ( $\gamma_s$ ) of NBSM ( $26.5 \pm 2.1$  mJ/m<sup>2</sup>) increased with both MM, C<sub>16</sub>POX<sub>15</sub> ( $42.6 \pm$   
 239  $13.5$  mJ/m<sup>2</sup>) and C<sub>18:2</sub>POX<sub>15</sub> ( $47.1 \pm 8.2$  mJ/m<sup>2</sup>). The apolar and electron donor components explained  
 240 these modifications. For both MM,  $\gamma^-$  increased while  $\gamma_{LW}$  was lowered thus reflecting a higher basic  
 241 monopolar behavior. MM C<sub>16</sub>POX<sub>15</sub> led to a higher increase of  $\gamma^-$  ( $72.2 \pm 11.6$  mJ/m<sup>2</sup>) compared to  
 242 MM C<sub>18:2</sub>POX<sub>15</sub> ( $51.1 \pm 17.8$  mJ/m<sup>2</sup>). Overall, once spread on the surface both POx from MM behaved  
 243 the same way with a modification of the surface energy through the electron donor component.

244 Regarding the LNC,  $\gamma_s$  significantly increased with C<sub>16</sub>POX<sub>15</sub> ( $39.6 \pm 7.1$  mJ/m<sup>2</sup>) and slightly increased  
 245 with C<sub>18:2</sub>POX<sub>15</sub> ( $28.6 \pm 4.9$  mJ/m<sup>2</sup>). The higher electron donor component ( $\gamma^-$ ) of C<sub>16</sub>POX<sub>15</sub> ( $69.9 \pm 10.9$   
 246 mJ/m<sup>2</sup>) compared to C<sub>18:2</sub>POX<sub>15</sub> ( $53.5 \pm 11.6$  mJ/m<sup>2</sup>) can explain this difference. Overall, the same  
 247 trends were observed as with MM.

248



249  
 250 *Figure 2: Free surface energy of NBSM after application of MM and LNC with C<sub>16</sub>POX<sub>15</sub> and C<sub>18:2</sub>POX<sub>15</sub>. Statistical*  
 251 *analysis was performed by a two-sample t-test between the NBSM and formulations (\*P < 0.05, \*\*P < 0.01,*  
 252 *\*\*\*P < 0.001)*

253 As a conclusion, with MM and LNC of both POx the NBSM became more monopolar basic meaning  
 254 more hydrophilic inducing more interactions with polar molecules. Higher surface energy was  
 255 reached with MM and LNC with saturated POx indicating a better affinity with hydrophilic and polar  
 256 compounds and spreading on NBSM [8]. To better understand the formulation behavior regarding  
 257 each surface energy components, the impact of each excipient was analyzed.

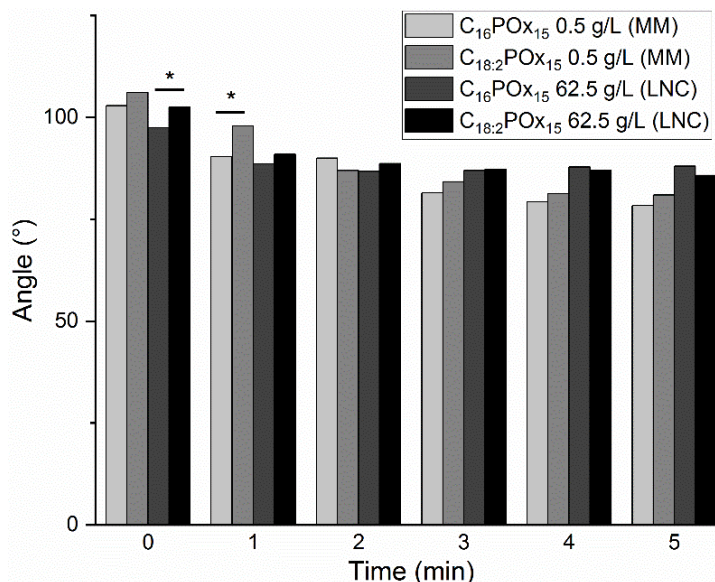
258

### 259 1.3.3 Impact of each component of the nanoformulations

260 Knowing that each component might influence the formulation behavior and explain the interactions  
 261 observed in the previous part, all excipients were analyzed on their own.

262 First, the contact angle of both POx solutions over 5 minutes was measured at the concentration  
 263 they were introduced in formulation: 0.5 g/L for MM and 62.5 g/L for LNC (Figure 3).

264 Overall, the contact angle did not decrease as much as for the formulations. However, two trends  
 265 appeared at 0-1 minute where the concentration dominated over POx and the opposite (POx  
 266 dominated over concentration) at 3-5 minutes when a plateau was reached. A significant difference  
 267 ( $P < 0.001$ ) for  $C_{16}POx_{15}$  from 0.5 g/L ( $78^\circ$ ) to 62.5 g/L ( $88^\circ$ ) was observed at 5 minutes and none for  
 268  $C_{18:2}POx_{15}$  (respectively  $81^\circ$  and  $86^\circ$ ). Therefore, no effect of alkyl chain was clearly noticed and a  
 269 slight effect of concentration with more hydrophilic modification at 0.5 g/L ( $\theta < 90^\circ$ ).



270  
 271 *Figure 3: Contact angle of  $C_{16}POx_{15}$  and  $C_{18:2}POx_{15}$  over 5 minutes as a function of time. Statistical*  
 272 *analysis was performed by a two-sample t-test between the same formulation with different POx (\* $P <$*   
 273 *0.05)*

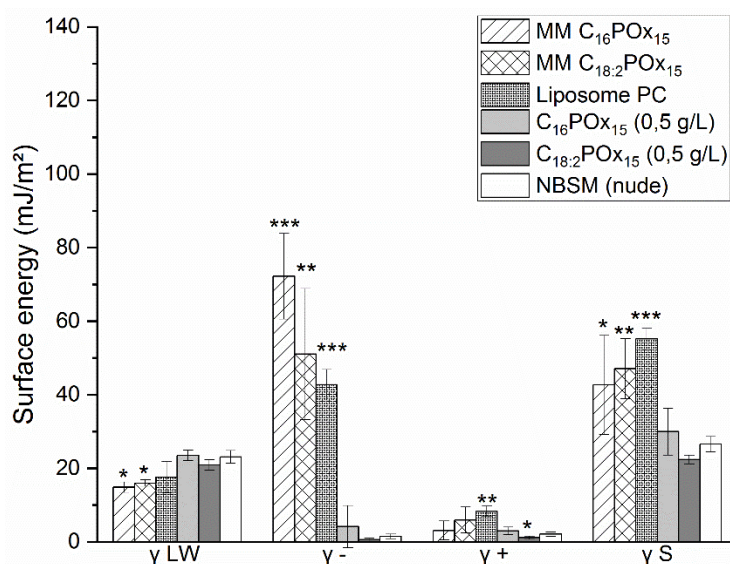
274 Secondly, the free surface energy was evaluated separately for MM and LNC with the formulation,  
 275 the POx and the excipients. Phospholipids were evaluated as liposomes at the concentration in  
 276 formulation. The surface energy of the NBSM with no formulation applied was measured and  
 277 considered as a reference for statistical analysis.

278

### 279 **Study of each component for mixed micelles**

280 Among the two MM formulations and their components ( $C_{16}POx_{15}$ ,  $C_{18:2}POx_{15}$ , and liposomes PC), the  
 281 PC give the higher surface energy  $\gamma_s$  ( $51.1 \pm 2.9$  mJ/m<sup>2</sup>). We do not observe any difference between  
 282 the intermediate values of MM formulations related to the corresponding POx. From all these results  
 283 we deduce that phospholipid PC was the component which mainly governed the interactions skin  
 284 model/nanoformulation.

285 Looking at the other  $\gamma_s$  components:  $\gamma^-$  and  $\gamma_{LW}$ , both POx had no significant difference with NBSM  
 286 reference. Nevertheless,  $C_{16}POx_{15}$  seemed to slightly impact more the NBSM properties. On the other  
 287 hand, liposome PC and both MM had significant increase of  $\gamma^-$  and slight of  $\gamma_{LW}$ . As a conclusion the  
 288 MM behavior was ruled by the phospholipids PC modifying the properties to more basic monopolar.  
 289 The main component of the formulation dominated the physicochemical interactions. This can be  
 290 linked with the phospholipids surfactant characteristics and capacity to modify skin properties as  
 291 demonstrated by Mavon et al. with the study on the sebum [6].



292  
 293 *Figure 4: Free surface energy of MM with each constituent for both POx. Statistical analysis was performed by a*  
 294 *two-sample t-test between NBSM and excipients (\*P < 0.05, \*\*P < 0.01, \*\*\*P < 0.001)*

295  
 296 **Study of each component for lipid nanocapsules:**

297 In the case of LNC, almost all components have a significant impact the  $\gamma_S$ , increasing the value from  
 298  $(26.5 \pm 2.1 \text{ mJ/m}^2)$  to  $(44.4 \pm 11.7 \text{ mJ/m}^2)$  with phospholipid S75,  $(47.6 \pm 0.3 \text{ mJ/m}^2)$  with Labrafac®,  
 299  $(39.7 \pm 7.1 \text{ mJ/m}^2)$  with LNC C<sub>16</sub>POx<sub>15</sub> and  $(40.4 \pm 4.1 \text{ mJ/m}^2)$  with C<sub>16</sub>POx<sub>15</sub>.

300 This increase of surface energy was mostly due to the drastic rise of  $\gamma^-$  as illustrated for liposome S75  
 301  $(122.1 \pm 6.2 \text{ mJ/m}^2)$ . The same trend was observed with LNC C<sub>16</sub>POx<sub>15</sub>  $(69.9 \pm 10.9 \text{ mJ/m}^2)$  and LNC  
 302 C<sub>18:2</sub>POx<sub>15</sub>  $(53.5 \pm 11.6 \text{ mJ/m}^2)$ . The electron donor behavior of LNC was this time governed by the  
 303 POx as C<sub>16</sub>POx<sub>15</sub>  $(72.1 \pm 7.2 \text{ mJ/m}^2)$  and C<sub>18:2</sub>POx<sub>15</sub>  $(57.1 \pm 13.3 \text{ mJ/m}^2)$ . A slight difference between  
 304 the two polymers was observed with a higher impact with the linear saturated POx triggered by the  
 305 very high electron donor behavior.

306 Regarding the apolar component, all excipients decreased value compared to NBSM except the oil  
 307 (Labrafac®) that had a major rise due to its apolar nature.

308 To conclude, both POx governed the LNC behavior as the main formulation component.

309

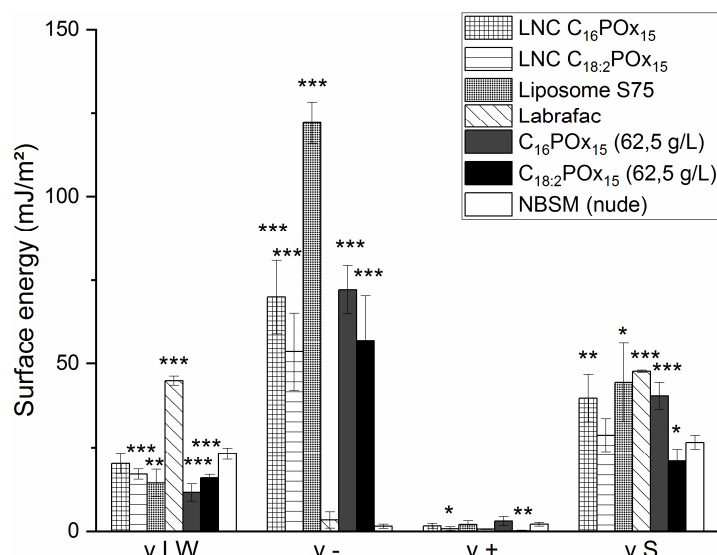


Figure 5: Free surface energy of LNC with each constituent for both POx. Statistical analysis was performed by a two-sample t-test between NBSM and excipients (\* $P < 0.05$ , \*\* $P < 0.01$ , \*\*\* $P < 0.001$ )

310  
311  
312  
313

The slight difference in between saturated and unsaturated POx might be explained by the air/liquid interfacial behavior with C<sub>16</sub>PO<sub>x15</sub> slightly more hydrophilic (CMC of 150 vs 100 mg/L) and a better effectivity (34 vs 32). Both formulations showed similar results in terms of surface energy and electron donor behavior. However, for MM the behavior was mainly governed by phospholipids and for LNC by POx. The difference might be explained with the difference of composition and structure. At high concentration (62.5 g/L), POx showed a pronounced electron donor behavior compared to none at low concentration (0.5 g/L). The morphology difference between MM and LNC might also impact the resulting formulation behavior. MM are made of an entanglement of phospholipids (PC) and POx that seem flexible and soft. On the contrary, LNC are highly ordered with oily core, phospholipids (S75) shell and POx corona therefore POx are localized in the outer part of the formulation, they interact directly with the surface. Moreover, the mechanical properties of LNC (rigid capsule) might lower the impact with less interaction capacity and during spreading on surface compared to MM. As the measured surface properties are very sensitive, a nanosized organization of each formulation might matter.

328  
329  
330  
331  
332  
333  
334  
335  
336  
337  
338  
339

It is difficult to compare these results with the literature as POx alone and formulated POx have never been tested on skin or on the NBSM and the surface physicochemistry is seldom studied. However, we can discuss with the experiments conducted by Mouzouvi et al on the lipid nanocapsules surface properties evaluated with drop tensiometry measurement [13]. Even if these LNC were based on PEG, the formulations were proved to lower the surface tension (35 mN/m) compared to the polymer alone (38 mN/m). Moreover, the high impact of surfactant on the LNC physicochemical properties was demonstrated. These findings are in agreement with the LNC POx. Indeed, the physicochemical interactions were improved with LNC POx compared to POx alone and the POx were shown to play a key role in these interactions.

## 340 **I.4 Conclusion**

341 This work investigated for the first time polyoxazolines influence on surface physicochemical  
342 properties formulated as well as in solution. As polyoxazolines have never been evaluated for topical  
343 application, a nonbiological skin surface model mimicking the human skin topography and sebum  
344 composition was first used. This tool provides insight on the tested polyoxazolines based  
345 nanoformulations capacity to potentially modify and penetrate the skin barrier. To conduct this  
346 study, two complementary parameters were assessed. First the spontaneous spreading on the  
347 surface model was observed showing the formulation affinity with the surface. Then, the evaluation  
348 of residual film after manual application of the formulations, reproducing the use conditions of  
349 topical products, reflected the modification of the surface physicochemical properties. Overall, mixed  
350 micelles and lipid nanocapsules spontaneous spreading was enhanced with the saturated  
351 polyoxazolines (C<sub>16</sub>POx<sub>15</sub>) indicating the impact of the polymer architecture on formulation  
352 spreading. Both formulations produced residual films able to modify the NBSM properties to more  
353 hydrophilic behavior (more electron donor  $\gamma^-$ ) thus enhancing the affinity with hydrophilic and polar  
354 molecules. Looking at the free surface energy components, both formulations behavior was  
355 governed by the main component. MM was led by the phospholipids (PC) and LNC by the POx, for  
356 this parameter, the structure of polyoxazolines had not influence. These new findings on amphiphilic  
357 polyoxazolines behavior on skin surface model highlighted their interesting capacity for topical  
358 delivery and these results will be confirmed on biological model such as human skin explant.

359

360

361

## 362 **ACKNOWLEDGEMENTS**

363 The authors would like to acknowledge Chimie Balard Cirimat Carnot Institute for the financial  
364 support as well as Ecole Doctorale Sciences Chimiques Balard (ED 459).

365

## 366 **References**

- 367 [1] J. van Smeden, M. Janssens, G.S. Gooris, J.A. Bouwstra, The important role of stratum corneum  
368 lipids for the cutaneous barrier function, *Biochimica et Biophysica Acta (BBA) - Molecular and Cell*  
369 *Biology of Lipids*, 1841 (2014) 295-313.
- 370 [2] J. Krutmann, A. Bouloc, G. Sore, B.A. Bernard, T. Passeron, The skin aging exposome, *Journal of*  
371 *Dermatological Science*, 85 (2017) 152-161.
- 372 [3] C. Baudouin, M. Charveron, R. Tarrow, Y. Gall, Environmental pollutants and skin cancer, *Cell*  
373 *Biology and Toxicology*, 18 (2002) 341-348.
- 374 [4] C.J. Van Oss, M.K. Chaudhury, R.J. Good, Interfacial Lifshitz-van der Waals and polar interactions  
375 in macroscopic systems, *Chemical Reviews*, 88 (1988) 927-941.
- 376 [5] A. Mavon, H. Zahouani, D. Redoules, P. Agache, Y. Gall, P. Humbert, Sebum and stratum corneum  
377 lipids increase human skin surface free energy as determined from contact angle measurements: A  
378 study on two anatomical sites, *Colloids and Surfaces B: Biointerfaces*, 8 (1997) 147-155.
- 379 [6] A. Mavon, D. Redoules, P. Humbert, P. Agache, Y. Gall, Changes in sebum levels and skin surface  
380 free energy components following skin surface washing, *Colloids and Surfaces B: Biointerfaces*, 10  
381 (1998) 243-250.
- 382 [7] F. Eudier, G. Savary, M. Grisel, C. Picard, Skin surface physico-chemistry: Characteristics, methods  
383 of measurement, influencing factors and future developments, *Advances in Colloid and Interface*  
384 *Science*, 264 (2019) 11-27.
- 385 [8] F. Eudier, M. Grisel, G. Savary, C. Picard, Design of a Lipid-Coated Polymeric Material Mimic  
386 Human Skin Surface Properties: a Performing Tool to Evaluate Skin Interaction with Topical Products,  
387 *Langmuir*, 36 (2020) 4582-4591.
- 388 [9] T. Lorson, M.M. Lübtow, E. Wegener, M.S. Haider, S. Borova, D. Nahm, R. Jordan, M. Sokolski-  
389 Papkov, A.V. Kabanov, R. Luxenhofer, Poly(2-oxazoline)s based biomaterials: A comprehensive and  
390 critical update, *Biomaterials*, 178 (2018) 204-280.
- 391 [10] L. Simon, N. Marcotte, J.M. Devoisselle, S. Bégu, V. Lapinte, Recent Advances and Prospects in  
392 NanoDrug Delivery Systems using Lipopolyoxazolines, *International Journal of Pharmaceutics*, (2020)  
393 119536.
- 394 [11] L. Simon, M. Vincent, S. Le Saux, V. Lapinte, N. Marcotte, M. Morille, C. Dorandeu, J.M.  
395 Devoisselle, S. Bégu, Polyoxazolines based mixed micelles as PEG free formulations for an effective  
396 quercetin antioxidant topical delivery, *International Journal of Pharmaceutics*, 570 (2019) 118516.
- 397 [12] L. Simon, V. Lapinte, L. Lionnard, N. Marcotte, M. Morille, A. Aouacheria, K. Kissa, J.M.  
398 Devoisselle, S. Bégu, Polyoxazolines based lipid nanocapsules for topical delivery of antioxidants,  
399 *International Journal of Pharmaceutics*, 579 (2020) 119126.
- 400 [13] C.R.A. Mouzouvi, A. Umerska, A.K. Bigot, P. Saulnier, Surface active properties of lipid  
401 nanocapsules, *PLoS One*, 12 (2017) e0179211.

402